Infrared Physics and Technology 108 (2020) 103361

Contents lists available at ScienceDirect

Infrared Physics & Technology

journal homepage: www.elsevier.com/locate/infrared

Rapid detection of moisture content and shrinkage ratio of dried carrot slices by using a multispectral imaging system

Peng Yu[a], Min Huang[a,*], Min Zhang[b], Qibing Zhu[a], Jianwei Qin[c]

[a] Key Laboratory of Advanced Process Control for Light Industry (Ministry of Education), Jiangnan University, Wuxi, Jiangsu 214122, China
[b] State Key Laboratory of Food Science and Technology, Jiangnan University, Wuxi, Jiangsu 214122, China
[c] USDA/ARS Environmental Microbial and Food Safety Laboratory, Beltsville Agricultural Research Center, Bldg., 303, BARC-East, 10300 Baltimore Ave., MD 20705-2350, USA

ARTICLE INFO

Keywords:
Carrot slice
Multispectral image
Drying
Moisture content
Shrinkage ratio

ABSTRACT

Carrot has high nutritional value and health-promoting effects and is popular among consumers. Real-time quality detection of dried carrot slices allows producers to adjust the process parameters of the drying device in time, thereby ensuring the final product quality and realizing energy conservation. Traditional methods of detecting moisture content and shrinkage ratio usually require a long measurement time, which is difficult to meet the needs of practical application. This investigated a rapid method based on a novel multispectral imaging system for acquiring multispectral images of samples in 25 wavebands over the spectral region between 675 and 975 nm at one time to detect moisture content and shrinkage ratio of dried carrot slices. The multispectral images of 600 carrot slice samples, which were dried at different times, were acquired using the multispectral imaging system. After extracting the spectral and GLCM features of the samples, prediction models were developed based on partial-least squares regression (PLSR) and least squares-support vector machines (LS-SVM) by using different feature combinations. Compared with PLSR models, LS-SVM models achieved better detection accuracy for moisture content and shrinkage ratio. The LS-SVM model obtained the following best results: coefficient of determination in prediction (Rp) = 0.942, root mean square error of prediction (RMSEP) = 0.0808%, and residual predictive deviation (RPD) = 2.636 for shrinkage ratio as well as Rp = 0.953, RMSEP = 0.0902%, and RPD = 3.271 for moisture content under static condition (without movement). The detection accuracy decreased with increasing movement speed of the test sample. When the movement speed of the sample was lower than 30 mm/s, the moisture content detected achieved satisfactory accuracy, with Rp = 0.941, RMSEP = 0.0981%, and RPD = 3.001. The novel multispectral imaging system shows potential for real-time detection of moisture and shrinkage of products during drying.

1. Introduction

Carrots are rich in a variety of essential nutrients for the human body and have edible and medicinal values. In addition to being used as fresh food, carrots are often processed into various snacks or raw food materials through drying to facilitate its preservation and increase its added value [1]. Moisture content and shrinkage ratio are two important indicators of the quality of dried carrots. Excessive moisture content may lead to the growth and reproduction of microorganisms in dried carrots, thereby increasing the risk of product decay; by contrast, low moisture content will affect the taste of dried carrot and lead to the destruction of some nutrients. The moisture loss in the drying process causes the capillary tube of the carrot to shrink, collapse, and curl under stress, resulting in obvious shrinkage of the material morphology on the macro level. Shrinkage ratio is an important sensory quality index and is not only closely related to subsequent processing, packaging, storage and transportation but also affects consumer purchase [2]. Conventional methods of detecting moisture content and shrinkage ratio (oven drying and volumetric ratio measurement) perform well in terms of reliability and accuracy. However, these methods are destructive, time consuming, and cannot easily realize the real-time or rapid detection of the quality of dried products. In the food drying industry, real-time or rapid detection of quality parameters ensures the product quality and help producers adjust the process parameters of equipment (such as drying time and power) in real time to optimize product quality and energy consumption [3]. Therefore, developing a rapid method for

* Corresponding author.
E-mail addresses: yupeng091333@163.com (P. Yu), huangmzqb@163.com (M. Huang), min@jiangnan.edu.cn (M. Zhang), zhuqib@163.com (Q. Zhu), jianwei.qin@ars.usda.gov (J. Qin).

https://doi.org/10.1016/j.infrared.2020.103361
Received 21 January 2020; Received in revised form 9 May 2020; Accepted 11 May 2020
Available online 15 May 2020

detection of moisture content and shrinkage ratio is necessary in the food drying industry.

The rapid and nondestructive detection technology of food quality has been widely studied to avoid the shortcomings of traditional detection methods. Machine vision and near-infrared spectroscopy are two common methods for food quality detection [4,5,6]. Machine vision mainly obtains image of objects in the visible wavelength range and can detect the shape and color changes of the target; however, its ability to detect chemical components (e.g., moisture content) is limited because chemical composition is mainly reflected in the infrared and near-infrared wavelength regions [7]. Although near-infrared spectroscopy is sensitive to detection of chemical composition, it can only measure a local area of the sample. The detection results based on local area information cannot truly reflect the spatial distribution of information due to uneven spatial distribution and changes in the chemical information of a measured sample [8].

Hyperspectral imaging technology is another nondestructive detection method that combines the advantages of machine vision and near-infrared spectroscopy. Hyperspectral imaging technology can obtain spectral and spatial information at the same time and provide a detailed information of the sample. In recent years, this technology has been applied to nondestructive detection of food product quality, particularly in detecting moisture and color of dried soybean [7] and beef during heating [9] and predicting physicochemical properties in mango [10]. The speed of detection is difficult to meet the speed of real-time detection needed in actual application given that a large amount of data of hyperspectral image are acquired and processed within a wide waveband range [11].

Multispectral image technology is introduced in quality inspection to improve the real-time performance of hyperspectral image detection. This technology only collects image information of the measured object in a small number of wavebands, thereby reducing the time and cost of image acquisition and processing and improving real-time detection for online application. Multispectral imaging is used for rapid detection of the surface defects of apples [12], moisture content in butter biscuits [13], and moisture content and water-holding capacity in cooked pork sausages [14].

Line scanning is the most commonly used approach for acquiring 3D hyperspectral/multispectral image cube. This method simultaneously records a whole line of spatial and spectral information corresponding to each spatial pixel in the line and acquires the spectral image information as the scanning line is along the moving direction of a moving platform [15,16]. Multispectral systems based on line scanning have time and cost requirements in data transmission, storage, and subsequent data processing over the hyperspectral system because only limited wavebands are collected. However, multispectral imaging system based on line scanning should perform exposure operation (integration of light intensity) on each detecting position (scanning line) in the moving direction; as such, multiple exposure operations (depending on the number of scanning lines) are required for collecting data of the whole sample. Each exposure time needs tens of milliseconds to ensure the signal-to-noise ratio of the signal, and the total time consumption of multiple exposures limits the real-time performance of the multispectral system. A new image acquisition method of single shot for multispectral imaging technology that differs from line scanning was developed. This method can record the spatial and spectral information of the whole samples simultaneously by using a large area detector with one exposure and can acquire spectral image in a short time. Thus, multispectral imaging technology based on single-shot method is a potential approach for online quality detection. However, the application of single-shot method in quality detection of agricultural products remains to be further studied due to its limited spatial resolution and small number of wavelengths.

This study aimed to explore the feasibility of using multispectral imaging technology to detect changes in the moisture content and shrinkage ratio of dried carrot slices. The specific objectives were to: (1) obtain multispectral images of carrot slices dried at different times in 25 wavebands over the spectral region between 675 and 975 nm; (2) develop PLSR and LS-SVM models for prediction of moisture content and shrinkage ratio in dried carrot slices by using spectral and textural features extracted from multispectral image and validate the model performance; and (3) analyze the effects of different feature combinations and moving speeds of the sample on the model performance.

2. Materials and methods

2.1. Dried carrot slices

Eighty fresh carrots were purchased from a local supermarket in Wuxi, China. After washing and peeling, the carrots were cut into slices with a diameter of 20 ± 2 mm and a thickness of 4 mm. A total of 600 experimental samples were prepared. The carrot slices were dried in a hot air drying oven at 100 °C for six gradients in 10–60 min with time interval of 10 min. One hundred carrot slices were dried at each time gradient. The dried samples were placed on the conveyor belt for multispectral image acquisition, and 300 samples (50 samples for each drying time) were used to determine the reference value of moisture content. The remaining samples were used to measure the reference value of shrinkage ratio.

2.2. Multispectral imaging system

The multispectral imaging system used in this study is shown in Fig. 1. The system consists of four parts: a light source, a sample transport platform, a computer with image acquisition software (HSI-25 bands-software), and a multispectral imaging unit. Two 150 W fiber halogen lamps were used as light source and symmetrically located on both sides of the camera to provide even light. The black conveyor belt was used as the sample transport platform, and its moving speed was adjusted by PLC controller. A snapshot mosaic multispectral imaging camera with pixel resolution of 2045 × 1080 (Model: cmv2k-SNM-25-600-1000, Isuzu Optics, Taiwan, China) was used to acquire the multispectral images of samples. The snapshot mosaic multispectral imaging camera can obtain spectral image at 25 wavebands over the spectral range of 675–975 nm (676, 690, 716, 730, 742, 757, 769, 782, 793, 806, 824, 836, 846, 857, 867, 877, 886, 895, 910, 918, 927, 932, 940, 946, and 952 nm). These 2045 × 1080 pixels can be divided into 409 × 216 mosaic areas with 5 × 5 pixels, and each mosaic area represents information of 25 wavebands from the measurement point of the sample. Therefore, multispectral images with a spatial resolution of 409 × 216 and 25 wavebands can be obtained at single shot. Compared with line-scanning hyperspectral cameras that are widely used in existing research, the snapshot mosaic multispectral imaging camera can significantly improve the speed of image acquisition and reduce the time and cost of data transmission and processing; as such, the latter is conducive to the development of a multispectral image acquisition and analytical system with satisfactory real-time performance [17].

The whole multispectral imaging system acquired image data in a closed black box, and the samples were placed in the preset acquisition area for spectral image acquisition; as such, the interference of external factors was reduced. The exposure time was set to 25 ms. The white and dark reference images were collected to compensate for the light source variation effect and dark noises. The corrected image can be expressed as follows [18]:

$$R_c = \frac{R_i - R_b}{R_w - R_b} \tag{1}$$

where R_c is the corrected multispectral images; R_i, R_w, and R_b are the multispectral images of the samples, whiteboard, and blackboard, respectively.

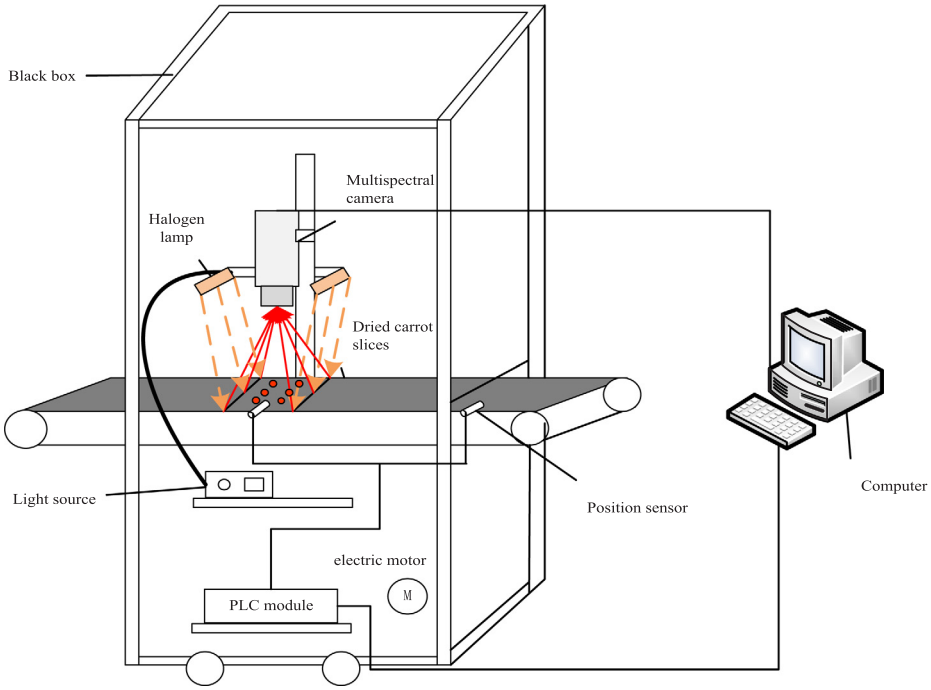

Fig. 1. Schematic of the multispectral image acquisition system.

2.3. Reference measurements of moisture content and shrinkage ratio

Moisture content in the dried carrot slices was expressed by wet base percentage (w.b) and measured by oven drying in accordance with the national standard (GB/T/8858-88, National Standard of China).

Shrinkage ratio was determined by the change in the volume of the carrot slices sample (cm^3) before and after drying. This parameter can be calculated by the following equation:

$$SR = \frac{V_d}{V_0} \tag{2}$$

where V_d and $V_0$are the volume of the sample (cm^3) before and after drying, respectively.

In this experiment, the volume of the carrot slice was calculated in accordance with the ratio of the weight to apparent relative density (ARD). ARD was determined in accordance with the national standard (GB/T6949-1998, National Standard of China). The calculation details of ARD can be obtained by referring to the experimental method described in the study [19] and the calculation formula is as follows:

$$ADR_{20}^{20} = \frac{m_1}{\left[\frac{m_2 + m_4 - m_3}{d_s}\right] - \left[\frac{m_2 - m_1}{d_{wax}}\right] \times d_w^{20}} \tag{3}$$

where m_1 and m_2 are the mass (g) of the sample before and after coating wax, respectively; m_3 is the density of the bottle plus sodium dodecyl sulfate–distilled water solution and the wax-coated sample; m_4 is the density of the bottle plus distilled water only; d_s, d_{was}, andd_w^{20} are the densities of 1 g/L sodium dodecyl sulfate solution (0.99847 $kgdm^{-3}$), the density of paraffin, and the density of distilled water at 20 ℃, approximating 1.00000 $kgdm^{-3}$.

2.4. Image feature extraction

The multispectral image contains information of the dried samples (called region of interest, ROI) and a large amount of irrelevant background information from the conveyor belt. Before extracting the multispectral image features of dried carrot slices, the ROI should be segmented from the whole image. In this experiment, the black conveyor belt has good color contrast with the dried carrot sample. Hence, an adaptive threshold segmentation method with simple operation and high accuracy was chosen to extract the image contour of the samples.

After ROI was segmented from the multispectral images, useful spectral and textural features should be extracted for subsequent data analysis. The spectral and textural features can reflect changes in chemical content and surface state of the dried carrot slices. Mean reflectance value (MV), entropy value (EV), relative divergence (RD), and standard deviation (SD) were calculated for each dried carrot slice. These features are related to the changes in spectral characteristics and texture information during drying [20]. MV, EV, RD, and SD are expressed in the following equations:

$$Mean\ Reflectance\ Value = \frac{1}{M_x * M_y} \sum_{i=1}^{M_x} \sum_{j=1}^{M_y} f(i,j) \tag{4}$$

$$Entropy\ Value = -\sum_{i=1}^{M_x} \sum_{j=1}^{M_y} h(i,j) \log_2 f(i,j) \tag{5}$$

$$h(i,j) = f(i,j) / \sum_{i=1}^{M_x} \sum_{j=1}^{M_y} f(i,j)$$

$$Standard\ Deviation = \sqrt{\frac{1}{M_x * M_y} \sum_{i=1}^{M_x} \sum_{j=1}^{M_y} (f(i,j) - \bar{f})^2} \tag{6}$$

$$Relative\ Divergence = \frac{1}{M_x * M_y} \sum_{i=1}^{M_x} \sum_{j=1}^{M_y} \frac{f(i,j) - f(a,b)}{\sqrt{(i-a)^2 + (j-b)^2}} \tag{7}$$

where $f(i,j)$ is the relative reflectance intensity of each pixel; M_x and M_y are the number of pixels in the horizontal and vertical directions, respectively; $\bar{f}$ is the average of relative reflectance intensity of all pixels; and (a, b) is the centroid coordinate of a sample.

In addition to extracting features from spectral images directly, gray-level co-occurrence matrix (GLCM) is also a potential method for expressing the characteristics of the multispectral image. GLCM is a texture analysis and statistical method based on the second-order statistics of the co-occurrence matrix. This method mainly measures the probability that two pixels in an image maintain the same gray level at a certain distance and a certain orientation. GLCM is useful in image

detection and shows potential for multispectral image prediction [21,22]. In the present study, five GLCM features (contrast or CT, correlation or CL, complexity or CP, entropy or EP, and homogeneity or HG were calculated from the GLCM when the distance is equal to 1 and under four different directions (0°, 45°, 90°, and 135°). The five textural features are expressed in the following equations:

$$Contrast = \sum_{i=0}^{X}\sum_{j=0}^{Y}(i-j)^2 p(i,j) \tag{8}$$

$$Correlation = \sum_{i=0}^{X}\sum_{j=0}^{Y}\frac{(i-\mu_i i)(j-\mu_j j)p(i,j)}{\sigma_i\sigma_j} \tag{9}$$

$$\mu_i = \sum_{i=0}^{X} i\sum_{j=0}^{Y} p(i,j)\mu_j = \sum_{j=0}^{Y} j\sum_{i=0}^{X} p(i,j)$$

$$\sigma_i = \sqrt{\sum_{i=0}^{X}(i-\mu_i)^2\sum_{j=0}^{Y} p(i,j)}\,,\ \sigma_j = \sqrt{\sum_{j=0}^{Y}(j-\mu_j)^2\sum_{i=0}^{X} p(i,j)}$$

$$Energy = \sum_{i=0}^{X}\sum_{j=0}^{Y} p(i,j) \tag{10}$$

$$Complexity = \sum_{i=0}^{X}\sum_{j=0}^{Y} p(i,j)\log(p(i,j)) \tag{11}$$

$$Homogeneity = \sum_{i=0}^{X}\sum_{j=0}^{Y}\frac{p(i,j)}{1+(i-j)^2} \tag{12}$$

where X , Y are the column and row numbers of GLCM and $p(i, j)$ is the gray level co-occurrence matrix.

For each GLCM, the values in the four directions were averaged. Finally, a total of 9 × 25 features (four spectral features and five GLCM statistical features for each waveband, and 25 wavebands for each sample) were obtained from the multispectral image and used to develop a model for predicting moisture content and shrinkage ratio of dried carrot slices.

2.5. Development of prediction models

PLSR and LS-SVM are two commonly used spectral modeling methods. In PSLR, the idea of data dimensionality reduction is used to deal with the problem of multiple collinearity among independent variables; as such, spectral information can be simplified and redundant noise can be removed [23,24]. In the present study, the appropriate number of potential variables of the model was determined by 10-fold cross validation. The optimal number of potential variables was determined when the root-mean- square error of the calibration set reached the minimum.

Support vector machine (SVM) constructs a nonlinear relationship model between input and output variables based on the idea of structural risk minimization. SVM shows good generalization ability when the small number of training samples was used for developing classification or regression models. LS-SVM is an improved version of SVM and modifies the inequality constraints in SVM to equality constraints. Thus, the algorithm efficiency of LS-SVM in terms of accuracy is better than that of SVM. In the present study, Gaussian function was used as the kernel function of LS-SVM. The optimal values of the hyper-parameter and kernel parameters were obtained using 10-fold cross validation [25].

2.6. Model performance indices

In this experiment, 300 dried carrot slices (six different drying times) were obtained to establish prediction models for moisture content and shrinkage ratio. The samples were randomly divided into calibration and prediction sets in accordance with the ratio of 3:1 (225 samples for calibration and 75 samples for prediction).The calibration and prediction procedure described above was repeated 10 times to achieve satisfactory results. After 10 runs, the average values of the correlation coefficient (i.e., Rc and Rp) and root-mean-square error for calibration and prediction models (RMSEC and RMSEP, respectively) were calculated to evaluate their performance. The smaller the correlation coefficient and the RMSE are, the more accurate the prediction results will be. Residual prediction deviation (RPD) was used to reflect the stability and robustness of the model. An RPD value between 2.5 and 3.0 indicates that the prediction model has good prediction accuracy but should be improved when used for actual quantitative prediction. An RPD higher than 3 indicates that the established prediction models have excellent prediction accuracy and can be applied to actual industrial production [26]. The prediction models were developed with the PLS-Toolbox 5.0 and LS-SVM V1.8 Toolbox using Matlab R2009b (The MathWorks Inc., USA). All of the above computations were performed a CPU platform (Intel(R) Pentium(R) CPU G2030 at 3.00 GHz with 4 GB of DDR3 RAM).

3. Results and discussion

3.1. Analysis of relative reflectance

Fig. 2 shows the representative mean reflectance curves, over the spectral range of 675–975 nm, of samples randomly selected from six dried sample groups, which dried with different times (10, 20, 30, 40, 50, and 60 min). The mean reflectance curves of carrot slices at different drying times had the similar pattern. The carrot slices dried for a short time (with a high moisture content) had high mean reflectance values. With prolonged drying time, the mean reflectance values decreased gradually possibly due to the evaporation of moisture and the changes in the color and micro-structure on the surface of the carrot slices during drying process. In the waveband range of approximately 940 nm, the mean reflectance spectrum decreased for all carrot slices. This condition is due to the stretching vibration of the O–H third stretching overtone of water molecules in the samples [27].

3.2. Measurement of moisture content and shrinkage ratio for carrot slices at different drying times

The moisture content of 300 dried carrot slices with different drying times (10–60 min) was determined by oven drying. The range of the moisture content measured by the instrument was 86.9%–6.7%. The average value of the moisture content was 46.4%, with a standard deviation of 22.4%. The shrinkage ratio of 300 carrot slices was measured by calculating the ratio of the sample volume before and after drying. The measured values were distributed within 81.9%–9.2%, with an average value of 28.6% and a standard deviation of 17.1%.

3.3. Prediction models for moisture content in carrot slices

Nine features (MV, EV, RD, SD, CT, CL, CP, EP, and HG) from multispectral images were obtained for each dried carrot slice. Different species of features combined with the actual moisture content and shrinkage ratio values were selected to establish PLSR and LS-SVM models based on the same calibration and prediction sets. The number of selected feature species was 1 to 9, and the features were randomly combined in accordance with the number of selected feature species. When n features were selected, all feature combinations were obtained exhaustively. The model prediction results were obtained and counted using each feature combination. Table 1 shows the best performance of PLSR and LS-SVM models in predicting moisture content by using different numbers of feature species. Compared with the prediction results of the PLSR model, those of the LS-SVM model were accurate when using the same calibration and prediction sets. The optimal prediction

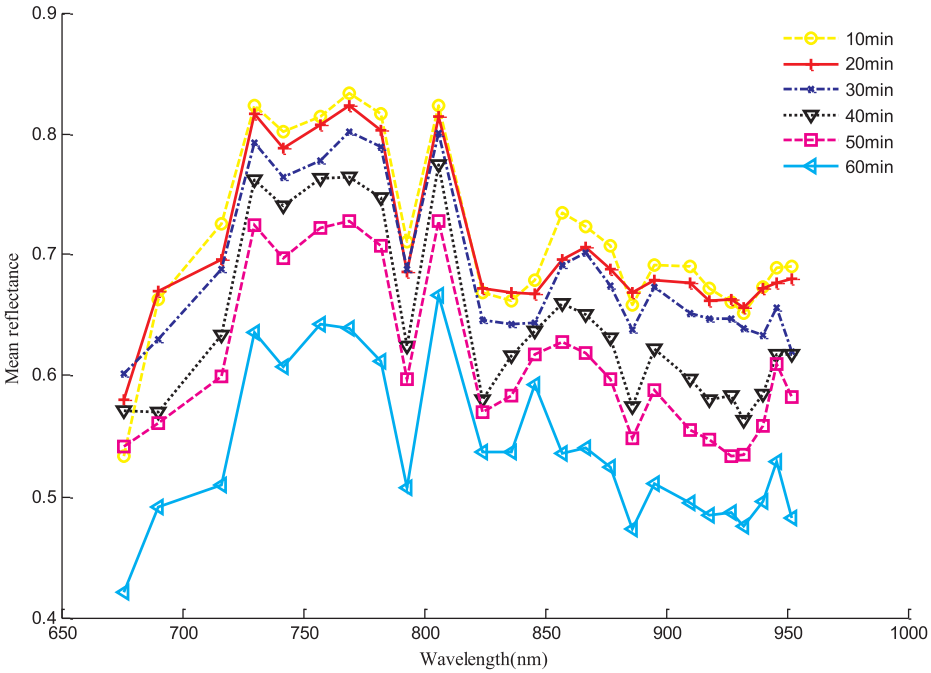

Fig. 2. Mean reflectance of six carrot slices at different drying times.

results of the moisture content improved with increasing number of selected features. When the number of features was one to five, the prediction effect was obviously improved. The degree of improvement of the prediction effect of the model slowed down when the number of species was six to nine. The CL feature was selected with the most times compared with the other selected features. Hence, the CL feature exhibited remarkable contribution for establishing moisture content prediction models.

In practical applications, the accuracy of the prediction results and the complexity of the data used to build a model should be considered. Compared with the LS-SVM model based on all the features, the accuracy of the LS-SVM model based on the five features were reduced by 2%, but the calculation time were reduced by about half(calculation time was about 2 s for 75 prediction samples). For rapid detection systems, less data collection and calculations were more helpful to meet real-time requirements in applications. As such, a LS-SVM model for predicting moisture content with five feature species (MV, EV, RD, CL, and CP) should be established. For the prediction set, the LS-SVM model based on selected five features achieved satisfactory average accuracy, with Rp = 0.953 and RMSEP = 0.0902. Fig. 3 shows the prediction results for moisture content versus the actual measurements for one of the 10 runs. The average value of RPD for the moisture content prediction models was 3.271, indicating satisfactory accuracy and stability of the model prediction results. Thus, the model can be applied for detection during production.

3.4. Prediction models for shrinkage ratio of carrot slices

Table 2 summarizes the prediction results of the shrinkage ratio of the samples by the PLSR and LS-SVM models established using different species of features. When the number of selected feature species was one to four, the prediction results of the two models tended to be satisfactory with increasing number of selected feature species. When the number of features was more than four, the prediction accuracy had a tendency to decrease. This tendency could be attributed to the increase in redundant information when the amount of data increased and is not conducive to establishing a prediction model. When selecting the same number of features, the LS-SVM model can obtain better prediction results than the PLSR model. According to the statistical results, the SD feature was selected most frequently when establishing prediction models for shrinkage ratio. The SD feature can reflect the change in the shrinkage ratio better than other features.

When four feature species (MV, SD, CT, EP) were selected for developing LS-SVM model, the prediction results were the most accurate and the time cost for 75 prediction samples were about 2.5 s, which reduced by 51% compared with using all features. For the prediction set, the average values of Rp and RMSEP (%) were 0.942 and 0.0808, respectively. Fig. 4 shows the prediction results for shrinkage ratio

Table 1
Prediction results of moisture content of dried carrot slices using LS-SVM and PLSR.

Number of feature species	LS-SVM				PLSR			
	Rp	RMSEP (%)	RPD	Feature	Rp	RMSEP (%)	RPD	Feature
1	0.929	0.113	2.687	CL	0.906	0.125	2.198	CL
2	0.936	0.103	2.856	CL, EP	0.922	0.115	2.452	CL, EP
3	0.945	0.0962	3.067	RD, CL, FP	0.926	0.112	2.600	EV, CL, CP
4	0.951	0.0918	3.209	EV, RD, CL, CP	0.935	0.105	2.731	EV, SD, CL, CP
5	0.953	0.0902	3.271	MV, EV, RD, CL, CP	0.937	0.103	2.780	EV, SD, CL, CP, EP
6	0.953	0.0893	3.285	RD, CT, CL, CP, EP, HG	0.936	0.104	2.766	EV, SD, CL, CP, EP, HG
7	0.954	0.0890	3.296	EV, RD, CT, CL,CP, EP, HG	0.935	0.105	2.745	EV, SD, CT, CL, CP, EP, HG
8	0.955	0.0888	3.323	MV, EV, RD, CT, CL, CP, EP, HG	0.938	0.101	2.810	MV, EV, SD, CT, CL, CP, EP, HG
9	0.956	0.0885	3.325	MV, EV, RD, SD, CT, CL, CP, EP, HG	0.940	0.0989	2.923	MV, EV, RD, SD, CT, CL, CP, EP, HG

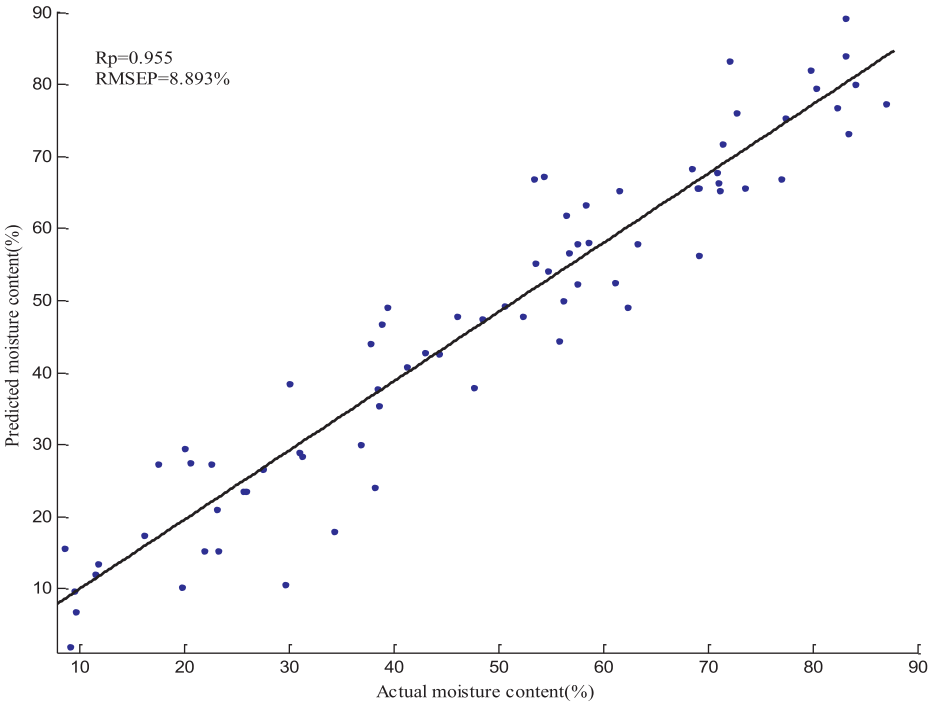

Fig. 3. Prediction of the moisture content of dried carrot slices using LS-SVM in one subset.

Table 2
Prediction results of shrinkage ratio of dried carrot slices using LS-SVM and PLSR.

Number of feature species	LS-SVM				PLSR			
	Rp	RMSEP (%)	RPD	Feature	Rp	RMSEP (%)	RPD	Feature
1	0.931	0.0855	2.463	SD	0.847	0.113	1.603	SD
2	0.939	0.0821	2.559	MV, SD	0.876	0.103	1.881	EV, SD
3	0.941	0.0814	2.593	MV, SD, HG	0.890	0.0981	2.029	MV, EV, SD
4	0.942	0.0808	2.636	MV, SD, CT, EP	0.871	0.0884	2.125	MV, EV, SD, EP
5	0.942	0.0806	2.631	MV, SD, CT, CL, EP	0.889	0.0972	1.999	MV, SD, CT, CP, EP
6	0.941	0.0815	2.614	MV, SD, CT, CL, CP, EP	0.893	0.0964	2.033	MV, SD, CT, CL, CP, HG
7	0.940	0.0814	2.596	MV, SD, CT, CL, CP, EP, HG	0.898	0.0943	2.076	MV, SD, RD, CT, CP, EP, HG
8	0.938	0.0821	2.584	MV, RD, SD, CT, CL, CP, EP, HG	0.892	0.0964	2.052	MV, RD, SD, RD, CT, CP, EP, HG
9	0.937	0.0822	2.583	MV, EV, RD, SD, CT, CL, CP, EP, HG	0.891	0.09590	2.041	MV, EV, RD, SD, CT, CL, CP, EP, HG

compared with the actual measurements for one of the 10 runs in one subset. The average value of RPD was 2.5, indicating that the LS-SVM model can predict the shrinkage ratio. However, some methods are needed to improve the prediction accuracy of the model for actual applications.

3.5. Detection of moisture content in dried carrot slices at different conveyor speeds

When the multispectral images of the dried carrot slices were obtained using the multispectral imaging acquisition system, the conveyor belt was in a stationary state. The multispectral image of the sample should be analyzed while the conveyor is moving to meet the requirements of the real-time and efficient quality inspection in production. Thus, the conveyor belt was continuously moved at different speeds without changing the equipment setting parameters. The dried carrot slices were placed from the entrance of the system on the moving conveyor belt. When the samples were transferred to the preset image acquisition area, the multispectral camera acquired and saved the multispectral images. During image acquisition, the conveyor was still moving. Based on the dynamic multispectral images obtained at different speeds, some spectral image features of the dried carrot slices were extracted in accordance with the above formulas.

Given that the RPD of the shrinkage ratio prediction models established above were all less than 3.0, the prediction results of the models were rough, and some necessary improvements were still needed to enhance the reliability of the prediction results. Therefore, this section only studied the establishment of prediction model of moisture content in dried carrot slices. A total of 300 carrot slices were used. The sample specifications and preparation methods were the same as those mentioned above. The actual value of moisture content was measured by oven drying. The acquired spectral images were calculated in accordance with the Formulas (4)–(6), (9) and (10) to obtain feature MV, EV, RD, CL, and CP, respectively. The conveyor belt moved at four different speeds (10, 20, 30, and 40 mm/s). Based on the prediction results of different models described, LS-SVM was chosen to determine moisture content. The average values of Rp and RMSEP(%) of the moisture content models established by the multispectral images acquired at different moving speeds are shown in Table 3.

The accuracy of the prediction results decreased with increasing speed of the conveyor when multispectral images were acquired dynamically. This result could be attributed to the increase in the speed of the conveyor belt, leading to an increase in the relative movement of the multispectral camera and the dried carrot slices increased within a fixed exposure time. The acquired multispectral image has issues, such as blurred images and missing information, which resulted in image

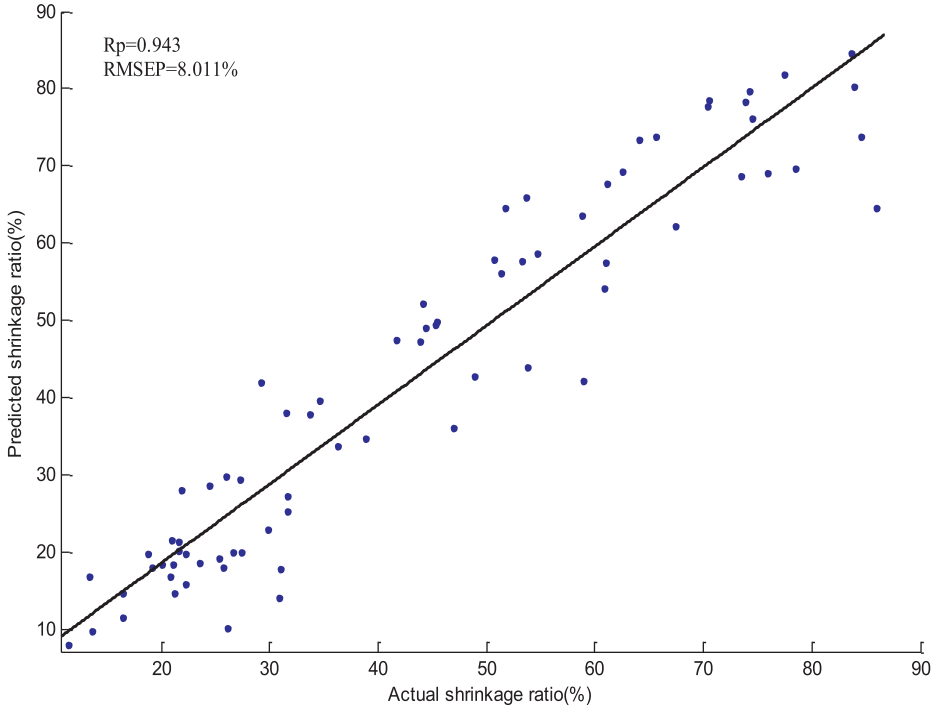

Fig. 4. Prediction of the shrinkage ratio of dried carrot slices using LS-SVM in one subset.

Table 3
Results of LS-SVM prediction model at different conveyor speeds.

Conveyor speed (mm/s)	Rp	RMSEP (%)	RPD
0	0.953	0.0902	3.271
10	0.950	0.0908	3.195
20	0.947	0.0941	3.099
30	0.941	0.0981	3.001
40	0.939	0.102	2.858

distortion. When the speed of the conveyor belt was less than 30 mm/s, the accuracy of the prediction model was satisfactory. The RPD values of the moisture content prediction models were greater than 3.0, indicating that the dynamic detection of moisture content in the moving state was achieved within 0–30 mm/s and ensuring the accuracy of the prediction results. Hence, this method can be used for rapid and accurate detection of moisture content in dried carrot slices in industrial production.

4. Conclusions

A rapid and nondestructive detection method through a multispectral imaging system based on single-shot method was proposed to assess the quality of carrot slices. This method can effectively acquire a 409 × 216 × 25 multispectral image in a short time. Spectral and GLCM features were extracted from the multispectral images of the dried carrot slices. LS-SVM showed better prediction results for moisture content and shrinkage ratio compared with PLSR. In view of the accuracy and real-time application of the prediction results, four features (MV, SD, CT, and EP) were selected to establish the LS-SVM model of shrinkage ratio, with Rp = 0.942, RMSEP (%) = 0.0808, and RPD = 2.636. In terms of shrinkage ratio, LS-SVM achieved good results for moisture content (Rp = 0.953, RMSEP (%) = 0.0902, and RPD = 3.271) by using five features (MV, EV, RD, CL, and CP). Multispectral images of continuously moving samples were acquired. When the moving speed of the conveyor belt was within 0–30 mm/s, the RPD of the moisture content prediction model was greater than 3.0 and corresponded to excellent prediction accuracy. Hence, the multispectral imaging system can be an effective method for rapid and nondestructive detection of quality of dried carrot slices for industrial applications.

Declaration of Competing Interest

The authors declare that they have no known competing financial interests or personal relationships that could have appeared to influence the work reported in this paper.

Acknowledgements

The authors gratefully acknowledge the financial support from the National Key R&D Program of China (Contract No. 2017YFD0400901), the National Natural Science Foundation of China (Grant no. 61775086, 61772240), and sponsored by the 111 Project (B12018).

References

[1] J. Gamboa-Santos, A.CSoria, M. Pérez-Mateos, J.A. Carrasco, A. Montilla, M. Villamiel, Vitamin C content and sensorial properties of dehydrated carrots blanched conventionally or by ultrasound, Food Chem. 136 (2013) 782-788.
[2] M. Roberto, S. Barbara, O.C. Stuart, A. Waseem, M, Riccardo, Postharvest monitoring of organic potato (cv. Anuschka) during hot-air drying using visible–NIR hyperspectral imaging, J. Sci. Food Agr, 98 (7) (2018) 2507-2517.
[3] Q. Hu, M. Zhang, A.S. Mujumdar, W. Du, J. Sun, Effects of different drying methods on the quality changes of granular edamame, Dry. Technol. 24 (8) (2006) 1025–1032.
[4] C. Shi, J. Qian, S. Han, B. Fan, X. Yang, X. Wu, Developping a machine vision system for simultaneous prediction of freshness indicators based on tilapia (Oreochromis niloticus) pupil and gill color during storage at 4 °C, Food Chem. 243 (2018) 134–140.
[5] L. Pan, R. Lu, Q. Zhu, J.M. McGrath, K. Tu, Measurement of moisture, soluble solids, sucrose content and mechanical properties in sugar beet using portable visible and near-infrared spectroscopy, Postharvest Biol. Tec. 102 (2015) 42–50.
[6] V.T.H. Tham, T. Inagaki, S. Tsuchikawa, A new approach based on a combination of capacitance and near-infrared spectroscopy for estimating the moisture content of timber, Wood Sci. Technol. 53 (3) (2019) 579–599.
[7] M. Huang, Q. Wang, M. Zhang, Q. Zhu, Prediction of moisture content and color for vegetable soybean during drying process based on multiple model fusion, J. Food Eng. 128 (2014) 24–30.
[8] M. Huang, X. Wan, M. Zhang, Q. Zhu, Detection of insect-damaged vegetable soybean using hyperspectral transmittance image, J. Food Eng. 116 (1) (2013) 45–49.

[9] Y. Liu, D. Sun, J. Cheng, Z. Han, Hyperspectral imaging sensing of changes in moisture content and color of beef during microwave heating process, Food Anal. Method. 11 (9) (2018) 2472–2484.
[10] P. Rungpichayapichet, M. Nagle, P. Yuwanbun, P. Khuwijitjaru, B. Mahayothee, J. Muller, Prediction mapping of physicochemical properties in mango by hyperspectral imaging, Biosyst. Eng. 159 (2017) 109–120.
[11] D. Wu, D. Sun, Potential of time series-hyperspectral imaging (TS-HSI) for non-invasive determination of microbial spoilage of salmon flesh, Talanta 111 (2013) 39–46.
[12] M.S. Kim, K.J. Lee, K. Chao, A.M. Lefcourt, W. Jun, D. Chan, Multispectral line-scan imaging system for simultaneous fluorescence and reflectance measurements of apples : multitask apple inspection system, J. Food Meas. Charact. 2 (2) (2008) 123–129.
[13] M.S. Andresen, S.B. Dissing, H. Løje, Quality assessment of butter cookies applying multispectral imaging, Food Sci. Nutr. 1 (1) (2013) 315–323.
[14] F. Ma, B. Zhang, W. Wang, P. Li, X. Niu, C. Chen, L. Zheng, Potential use of multispectral imaging technology to identify moisture content and water-holding capacity in cooked pork sausages, J. Sci. Food Agr. 98 (5) (2018) 1832–1838.
[15] K. Chao, C. Yang, Y. Chen, M.S. Kim, D. Chan, Hyperspectral-multispectral line-scan imaging system for automated poultry carcass inspection applications for food safety, Poultry Sci. 86 (11) (2007) 2450–2460.
[16] B. Park, S.C. Yoon, W.R. Windham, K.C. Lawrence, M.S. Kim, Line-scan hyperspectral imaging for real-time in-line poultry fecal detection, J. Food Meas. Charact. 5 (1) (2011) 25–32.
[17] G. Tzagkarakis, W. Charle, P. Tsakalides, Data compression for snapshot mosaic hyperspectral image sensors. In Proceedings of the IEEE 2016 24th European Signal Processing Conference (EUSIPCO), Budapest, Hungary, 9 Aug 9 - Sep 16 2016.
[18] N.D.T. Nghia, C.D. Jean, S. Woute, Cross-polarized VNIR hyperspectral reflectance imaging for non-destructive quality evaluation of dried banana slices, drying process monitoring and control, J. Food Eng. 238 (2018) 85–94.
[19] Y. Wang, M. Zhang, A.S. Mujumdar, K.J. Mothibe, S.M.R. Azam, Study of drying uniformity in pulsed spouted microwave-vacuum drying of stem lettuce slices with regard to product quality, Dry. Technol. 31 (1) (2013) 91–101.
[20] Y. Ma, M. Huang, B. Yang, Q. Zhu, Automatic threshold method and optimal wavelength selection for insect-damaged vegetable soybean detection using hyperspectral images, Comput. Electron. Agr. 106 (2014) 102–110.
[21] J. Gao, X. Li, F. Zhu, Y. He, Application of hyperspectral imaging technology to discriminate different geographical origins of Jatropha curcas L. seeds, Comput. Electron. Agr. 99 (2013) 186–193.
[22] G. Hamid, M. Golasa, F. Hakimeh, Spectroscopic studies on Solvatochromism of mixed-chelate copper(II) complexes using MLR technique, Spectrochim. Acta. A. 85 (1) (2012) 25–30.
[23] F. Mendoza, R. Lu, D.W. Ariana, H. Cen, B. Bailey, Integrated spectral and image analysis of hyperspectral scattering data for prediction of apple fruit firmness and soluble solids content, Postharvest Biol. Tec. 62 (2) (2011) 149–160.
[24] H. Yu, H. Liu, N. Wang, Y. Yang, A. Shi, L. Liu, H. Hu, R.I. Mzimbiri, Q. Wang, Rapid and visual measurement of fat content in peanuts by using the hyperspectral imaging technique with chemometrics, Anal. Methods. 8 (2016) 7482–7492.
[25] M.M. Adankon, M. Cheriet, Model selection for the LS-SVM, Application to handwriting recognition, Pattern Recogn. 42 (12) (2009) 3264–3270.
[26] Y. Kamruzzaman, S. Makino, Oshita, Rapid and non-destructive detection of chicken adulteration in minced beef using visible near-infrared hyperspectral imaging and machine learning, J. Food Eng. 170 (2016) 8–15.
[27] Y. Wei, F. Wu, J. Xu, J. Sha, Z. Zhao, Y. He, X. Li, Visual detection of the moisture content of tea leaves with hyperspectral imaging technology, J. Food Eng. 248 (2019) 89–96.

Min Huang is a professor in the school of Internet of Things Engineering at the Jiangnan University. Her research interests include nondestructive detection, modeling, and analysis of agricultural products and food quality.